A REVIEW OF NEW MANIFESTATIONS OF COLLECTIVE EFFECTS

F. Ruggiero, CERN, Geneva, Switzerland

Abstract

The design of high performance 'factories', large hadron colliders and synchrotron light sources calls for a large number of high intensity bunches. This imposes feedback systems and a tight impedance budget to control conventional instabilities, some of which are differently emphasised depending on the ongoing evolution of beam parameters. Ion trapping, for example, is no longer reported as a problem for the new generation of very low emittance electron storage rings. However new mechanisms appear, such as the fast ion instability for electron beams and the build-up of electron clouds for positron or proton beams. We review these new manifestations of collective phenomena, essentially related to the single-pass interaction of a bunch train with foreign or 'gaijin' particles, and discuss their dependence on several machine parameters such as bunch intensity and spacing. We also summarise possible cures and positive as well as negative experimental evidence in existing accelerators.

1 INTRODUCTION

The concept of gaijin particles [1] implies that they are foreign and can do damage to the stored native beam. For example conventional ion effects are known for many years: in this case the gaijin particles are positive ions generated by beam-gas collisions and trapped over many turns in the negative potential of an electron or antiproton beam. For a beam with r.m.s. sizes $\sigma_{\rm x}$, $\sigma_{\rm y}$, bunch population $N_{\rm b}$ and *uniform* spacing $L_{\rm sep}$, only ions with atomic mass number $A > N_{\rm b} r_{\rm p} L_{\rm sep}/2\sigma_{\rm y}(\sigma_{\rm x}+\sigma_{\rm y})$ can be permanently trapped. Therefore ion trapping becomes more difficult for low emittance beams. It gives rise to tune shifts and increased tune spread (which may help stability), but can cause transverse emittance blow-up and poor beam lifetime. A sufficiently long clearing gap in the bunch structure, however, can cure the problem. On the contrary, such a gap has only a limited effect in the case of the Fast Beam-Ion Instability (FBII), first predicted and analysed in several theoretical studies [2]–[6] and then observed in experiments recently carried out at ALS [7]–[10], TRISTAN AR [11, 12] and PLS [13, 14]. For high beam intensity and small emittances this instability can arise even when the ions are not trapped over multiple beam passages. Therefore the FBII is potentially dangerous also for future linear accelerators or transfer lines; it is reminiscent of beam break-up in linacs. The single-pass character of the FBII and of the new electron instabilities that may affect positron or proton beams is associated with a broad spectrum of betatron sidebands, in contrast to conventional coupled-bunch instabilities caused by the narrow-band impedance.

2 ION EFFECTS

Interesting ion effects have been recently observed in the SLAC electron damping ring, with one or two bunches, under exceptionally poor vacuum conditions [17]. The classical theory for the onset of ion-induced instability [18] does not seem to explain why the instability disappeared at low current. Indeed the vertical tune spread $\Delta Q_y^{\rm rms}$ required to suppress the instability by Landau damping should be about four times the coherent tune shift due to ions (about 0.025), while the measured r.m.s. tune spreads were much smaller (typically below 0.002). However, the r.m.s. tune spread may not be appropriate to estimate Landau damping in view of the 'Christmas-tree' like ion distribution [19] depicted in Fig. 1, which shows the vertical density for *cold* trapped ions in a flat Gaussian beam obtained by solving the Liouville equation and neglecting space charge effects.

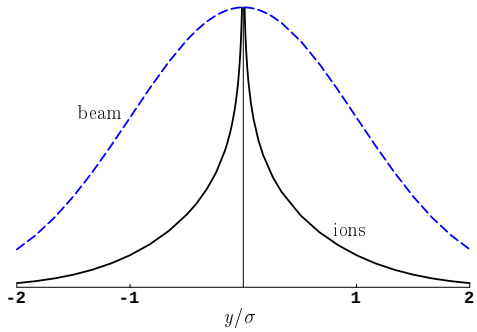

Figure 1: Vertical density (arbitrary units) of cold ions trapped in a flat Gaussian beam [19]: the r.m.s. size of the ion distribution is $\sigma/\sqrt{2}$, but the core is significantly narrower than the beam and has a width proportional to $\sqrt{\sigma}$, with tails decreasing as the beam density divided by y.

2.1 Fast Beam-Ion Instability

The FBII can be seen as a mechanism that amplifies the transverse motion of the first bunch and propagates it to subsequent bunches in the train. Therefore any damping mechanism, even weaker than the instability growth rate, will damp the oscillations of the first bunch (not driven by ions) and subsequently of all other bunches. The FBII is thus only a transient effect, but the oscillation amplitude temporarily reached by bunches in the tail of the train can be of several σ's and may degrade beam emittance and/or lifetime. The basic theory is contained in Refs. [2]–[6], which discuss the transient ion build-up along a bunch train, the effect of ion decoherence and of variations of the betatron function around the ring, and saturation effects at large oscillation amplitudes. More recent studies have addressed the problem of feedback and noise [15, 16].

For small offsets between beam centroid y_b and ion centroid y_i, the *linearised* equation of motion for the electron beam can be written

$$\frac{\mathrm{d}^2 y_\mathrm{b}}{\mathrm{d}t^2} + {\omega_\beta}^2 y_\mathrm{b} = 2\omega_\beta \Delta\omega_\beta \, (y_\mathrm{i} - y_\mathrm{b}) \qquad (1)$$

and describes a free betatron oscillation driven by the beam-ion interaction, characterised by a betatron frequency shift $\Delta\omega_\beta \ll \omega_\beta$. Since ions are continuously produced by collisions with the residual gas, the local frequency shift $\Delta\omega_\beta = \omega_o \Delta Q_\beta^\mathrm{tr} \, z/L_\mathrm{tr}$ increases linearly with the distance $z = ct - s$ from the head of the bunch train: here $\omega_o = c/R$ is the angular revolution frequency around the ring of radius R and L_tr is the length of the bunch train. Assuming a Gaussian beam distribution and also a *Gaussian ion distribution* (with r.m.s. sizes smaller by a factor $\sqrt{2}$), for *rigid* dipole oscillations the betatron tune shift at the end of the train is $\Delta Q_\beta^\mathrm{tr} = (\kappa L_\mathrm{tr} R^2)/(2Q_\beta)$, where the coefficient

$$\kappa = \frac{4\dot{\lambda}_\mathrm{ion} r_\mathrm{e}}{3\gamma c \sigma_\mathrm{y}(\sigma_\mathrm{x} + \sigma_\mathrm{y})}$$

is proportional to the average gas ionization rate per unit length $\dot{\lambda}_\mathrm{ion} \simeq 9 \times 10^8 \, (\sigma_\mathrm{i}/\mathrm{Mbarn}) \, (p_\mathrm{gas}/\mathrm{Torr}) \, N_\mathrm{b}/L_\mathrm{sep}$. For a typical ionization cross section $\sigma_\mathrm{i} = 2$ Mbarn (CO at 40 GeV) and a gas pressure $p_\mathrm{gas} = 1$ nTorr, the linear ion density after the passage of a bunch with $N_\mathrm{b} = 3 \times 10^{10}$ electrons increases by $\Delta\lambda_\mathrm{ion} \sim 180$ ions/m.

The linearised equation of motion for a ion produced at rest with initial displacement equal to the beam offset $y_\mathrm{b}(s,t')$ at time t' is

$$\frac{\partial^2 \tilde{y}_\mathrm{i}(s,t;t')}{\partial t^2} + {\omega_\mathrm{i}}^2 (\tilde{y}_\mathrm{i}(s,t;t') - y_\mathrm{b}(s,t)) = 0,$$

where $\omega_\mathrm{i} = \sqrt{\frac{4 N_\mathrm{b} r_\mathrm{p}}{3 L_\mathrm{sep} \sigma_\mathrm{y} (\sigma_\mathrm{x} + \sigma_\mathrm{y}) A}}$ is the ion oscillation frequency. The solution is [5]

$$\tilde{y}_\mathrm{i}(s,t;t') = y_\mathrm{b}(s,t) - \int_{t'}^{t} \mathrm{d}t'' \, \frac{\partial y_\mathrm{b}(s,t'')}{\partial t''} \cos\omega_\mathrm{i}(t - t'')$$

and the ion centroid is the average over the time interval $t - s/c$

$$y_\mathrm{i}(s,t) = \frac{1}{t - s/c} \int_{s/c}^{t} \mathrm{d}t' \, \tilde{y}_\mathrm{i}(s,t;t'). \qquad (2)$$

Therefore, combining Eqs. (1), (2) and using the new time variable z, the governing equation for linearised beam-ion oscillations $y(s,z) = y_\mathrm{b}(s, s+z)$ becomes

$$\frac{\partial^2 y(s,z)}{\partial s^2} + \frac{{\omega_\beta}^2}{c^2} y(s,z) = -\kappa \int_0^z \mathrm{d}z' z' \frac{\partial y(s,z')}{\partial z'} \cos\omega_\mathrm{i}(z - z').$$

The most unstable solution can be represented as a resonant wave propagating in the beam with a slowly varying amplitude $\mathcal{A}$

$$y(s,z) = \mathrm{Re}\, \mathcal{A}(s,z) \exp\left[\frac{i}{c}(\omega_\mathrm{i} z - \omega_\beta s)\right]. \qquad (3)$$

Averaging over rapid oscillations, the equation for A reads

$$\frac{\partial^2 \mathcal{A}(s,z)}{\partial s \, \partial z} = \frac{\kappa\omega_\mathrm{i}}{4\omega_\beta} \, z \mathcal{A}(s,z)$$

and has solution $\mathcal{A}(s,z) \propto I_o\left((z/L_\mathrm{tr})\sqrt{s/c\tau}\right)$, where the characteristic time τ of the linear instability, given by

$$\tau = \frac{2\omega_\beta}{c\kappa\omega_\mathrm{i} {L_\mathrm{tr}}^2},$$

scales as $\tau^{-1} \sim p_\mathrm{gas} \, {k_\mathrm{b}}^2 \sqrt{{N_\mathrm{b}}^3 L_\mathrm{sep}/({\sigma_\mathrm{y}}^3 (\sigma_\mathrm{x} + \sigma_\mathrm{y})^3 A)}$. Typical values of τ for future B-factories are in the μs range. Asymptotically, for large s, the oscillation amplitude is $\mathcal{A} \propto \exp\left((z/L_\mathrm{tr})\sqrt{s/c\tau}\right)$: the ratio z/L_tr is proportional to the bunch number in the train, so the oscillation amplitude increases exponentially along the bunch train, but depends on s (i.e., on the turn number) 'quasi-exponentially' and scales as the product $s \, p_\mathrm{gas}$.

2.2 Observations and cures

Observations of the FBII during dedicated machine experiments, in which either helium or nitrogen gas was intentionally leaked into the vacuum chamber, are in qualitative agreement with theoretical predictions and simulation results. A significant increase of the vertical beam size is observed in a regime where multi-turn ion trapping is not expected, a wide spectrum of betatron sidebands appears and the oscillation amplitude in the tail of the bunch train is larger than in the head. This is convincing evidence of a transient ion effect. However the measured phase advance of the bunch oscillation along the bunch train [12], proportional to the ion frequency according to Eq. (3), is about half of the value predicted by the linear theory for rigid oscillations of Gaussian beams. Also the measured variation of betatron tune along the bunch train is sometime negative, rather than positive, and points to possible additional effects of conventional short-range wakefields.

Variations of the betatron function along the ring can give rise to a significant spread $\delta\omega_\mathrm{i}$ of the ion frequency. As a consequence the beam oscillation amplitude grows exponentially with the number of turns [3] and the instability rise time is multiplied by $2\,\delta\omega_\mathrm{i} L_\mathrm{tr}/c$, reaching typical values in the ms rather than μs range for future B-factories. A fast feedback system is then effective in damping the instability without beam quality degradation [15, 16]. Another possible cure is Landau damping, induced either by octupoles or by a large chromaticity. This may be the reason why no systematic observation of FBII is reported in the ESRF, although a beam halo is sometimes observed at start-up in presence of local pressure bumps ($p_\mathrm{gas} \sim 10^{-6}$ Torr) and both for 1/3 or 2/3 bunch filling pattern [20].

3 ELECTRON CLOUD EFFECTS

Synchrotron radiation from positron or proton bunches creates photoelectrons at the pipe wall. These photoelectrons

are pulled towards the positively charged bunch. When they hit the opposite wall, they generate secondary electrons which can in turn be accelerated by the next bunch if they are slow enough to survive. Depending on surface reflectivity, photo-emission and secondary-emission yields, this mechanism can lead to the fast build-up of an electron cloud only limited by space charge effects, with potential implications for beam stability (the predicted rise times are 0.1 ms for the KEKB LER and 0.3 ms for the PEP-II LER) and heat load on the cold LHC beam screen.

For short bunch spacings, photoelectrons may interact with several bunches before hitting the opposite wall; this *photoelectron dominated regime* was originally studied by Ohmi [21] to explain a coupled-bunch instability observed at the KEK Photon Factory [22], where conventional electromagnetic wakefields could not account for the observed intensity dependent shift of the vertical betatron sidebands. For low wall reflectivity, the initial position of primary photoelectrons depends on the vertical offset of the first bunch. In field-free regions, they are accelerated by the bunch and form a horizontal strip; the next bunch experiences a vertical force proportional to the offset of the first bunch, therefore the photoelectron cloud behaves like a wakefield.

Further observations at BEPC [23] have confirmed a fast vertical instability of the positron beam with low threshold current, strongly dependent on bunch separation and chromaticity, different from the instability observed at CESR [24] and successfully explained in terms of electrons trapped by the dipole magnetic field combined with the static quadrupole electric field from Distributed Ion Pump leakage. More recently, direct evidence for electron effects in the APS [25] has been obtained by measuring a large variation of the electron current collected by a probe with the intensity of the positron beam.

Electron cloud effects are expected in the positron ring of the Frascati Φ-factory. The maximum beam current accumulated in multi-bunch mode is about 250 mA, i.e. 5% of the nominal value, limited by residual gas pressure in the (aluminium) vacuum chamber, but no evidence of electron cloud instability has been detected so far. Simulations by M. Furman, assuming unit reflectivity, unit photo-electron yield, 99% efficiency of the ante-chamber slot and 5% of the nominal beam current, indicate a transverse instability rise time of about 10 ms in the dipole magnets. Simulations by F. Zimmermann under similar conditions for the field-free regions indicate a rise time of about 2 ms. This should be compared to the betatron damping time of 36 ms. The assumption of *unit* photo-electron yield is probably pessimistic, since the critical energy of the synchrotron radiation in the bends is only 210 eV: the instability growth rate scales about linearly with the photo-electron yield and this may explain the discrepancy between simulations and observation.

The linear photon flux due to synchrotron radiation in the LHC is $\Phi_\gamma \simeq 10^{17} \frac{\text{photons}}{\text{m}\cdot\text{s}}$. The critical energy of these photons is $\varepsilon_{\rm cr} \simeq 45$ eV, i.e., well above the work function for copper. A first estimate [28] of the corresponding heat load on the cold beam screen gave a linear power of about 0.2 W/m comparable to the heat load due to synchrotron radiation. This estimate does not include a possible electron cloud build-up associated with secondary emission, which can significantly increase the power deposition and, according to earlier simulations [27], can lead to a very fast horizontal multi-bunch instability. An intensive research program [26] has been set up at CERN to measure the relevant physical quantities and to validate analytic estimates and simulation results: a fairly complete account of the contributions to this 'crash program' can be found in Refs. [27]–[44].

For a uniform illumination of the beam screen, corresponding to high surface reflectivity, the average energy gain in a dipole magnet is smaller by a factor two compared to a field-free region, since only the vertical component of the beam force is effective in accelerating the electrons. Indeed they spiral along the vertical magnetic field lines with typical Larmor radii of a few μm and perform about a hundred cyclotron rotations during a bunch passage. On the other hand, the heat load in a dipole magnet is drastically reduced if the screen reflectivity is much smaller than unity: in this case, photoelectrons and secondary electrons are produced only near the horizontal plane, where the vertical component of the beam force is very small. A simple geometrical solution to reduce both the photoelectric yield and the forward scattered reflectivity, is to arrange near perpendicular incidence of the photons. A structure which has been studied is a ribbed, sawtooth shaped Cu surface in the median plane where photons impinge at near perpendicular incidence. A photoelectron yield per adsorbed photon of 0.05 and a forward scattered photon reflectivity of about 2% were measured from this surface [32].

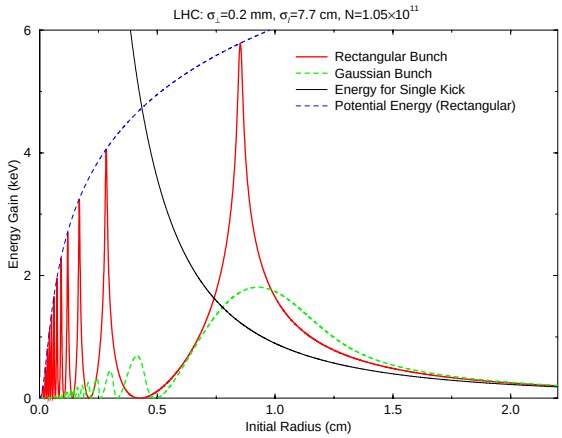

Figure 2: Electron energy gain (keV) versus initial radial offset (cm) for the LHC: the solid curve diverging at small radial offsets is the kick approximation, the two lower curves refer to Gaussian and rectangular longitudinal bunch distributions. Here the peaks correspond to electrons temporarily trapped in the bunch potential, performing an integer number of oscillations plus one quarter [31].

In kick approximation, i.e. neglecting the electron motion during the passage of the proton bunch, the maximum

energy gain of an electron initially at rest with radial offset a from the beam axis is independent of the bunch length and given by $\varepsilon_{\max} = 2m_{\rm e}c^2{N_{\rm b}}^2r_{\rm e}^2/a^2$, where c is the speed of light, $m_{\rm e}$ the electron mass and $r_{\rm e}$ its classical radius. For a photoelectron starting at the wall $a \simeq 2$ cm of the LHC beam screen, $\varepsilon_{\max} \simeq 200$ eV and the corresponding travel time to the opposite wall is about 5 ns, i.e., significantly shorter than the 25 ns bunch spacing. The LHC is therefore in a very different regime from B-factories. When the next bunch arrives, there is a relatively uniform distribution of photoelectrons (plus secondary electrons) in the screen cross section: the energy gain can reach a few keV and these fast particles hit very quickly the screen walls, producing low energy secondary electrons. However, for a correct modelling of the electron motion during the bunch passage [31] one has to cut the bunch into several transverse slices (typically 50). This is important for electrons near the beam axis, when the energy gain in kick approximation is largely overestimated (see Fig. 2), and is a key ingredient in all recent simulations of the LHC electron cloud dynamics [34, 35, 36, 40, 43].

3.1 *Electron Cloud build-up in the LHC*

Here I shortly review the theory of electron cloud build-up recently developed at CERN by G. Stupakov [39] and use his quasi-analytic results to discuss the dependence of the *critical* secondary emission yield $\delta_{\rm cr}$ on the bunch population $N_{\rm b}$ and bunch separation $L_{\rm sep} = ct_{\rm sep}$.

The average number of secondary electrons emitted when a primary electron of energy W hits a metal surface with incidence angle θ from the normal can be written [45]

$$\delta_{\rm SEY}(W,\theta) = \frac{\delta_{\max}}{\cos\theta}\, h\left(\frac{W}{W_o}\right), \qquad (4)$$

where the maximum yield $\delta_{\max}$, corresponding to a primary electron energy W_o typically around 400 eV, is a characteristic of the metal ($\delta_{\max} = 1.3 \div 2.5$ for copper, depending on surface preparation and *electron dose*), while h is a universal function having the phenomenological expression $h(\xi) = 1.11\,\xi^{-0.35}\left(1 - e^{-2.3\,\xi^{1.35}}\right)$.

With some simplifying assumptions about the shape of the beam screen (circular with radius a) and the velocity distribution of the secondary electrons (half-Maxwellian with characteristic energy $W_{\rm s} = mv_{\rm s}^2$), it is possible to solve analytically the Vlasov equation describing the free drift of these electrons along the vertical magnetic field lines in a bending dipole. The initial phase space distribution for secondary electrons produced at the screen wall with vertical coordinate $y_o(x) = \sqrt{a^2 - x^2}$ is

$$f_{\rm e}^{(o)}(x,y,v) = n_o(x)\sqrt{\frac{2m}{\pi W_{\rm s}}}e^{-mv^2/2W_{\rm s}}\delta(y \pm y_o(x)),$$

where $n_o(x)$ denotes the initial electron surface density at the screen wall projected on the horizontal plane (particles per unit area in the horizontal plane) and the velocity $v > 0$ is directed from the wall towards the beam axis.

The vertical drift velocity along the magnetic field lines is $v_y = \mp v y_o/a$ and the evolution of the electron cloud density $n_{\rm e}(x,y,t)$ during the time interval between two subsequent bunches is given by

$$n_{\rm e}(x,y,t) = \frac{2n_o(x)}{tv_{\rm s}y_o(x)/a}\left[\lambda^-(x,y,t) + \lambda^+(x,y,t)\right],$$

where the two terms in square brackets account for electrons drifting away from the upper or lower parts of the screen walls, respectively, and $\lambda^{\mp}(x,y,t) = \frac{1}{\sqrt{2\pi}}\exp\left[-\frac{1}{2}\left(\frac{y \mp y_o(x)}{tv_{\rm s}y_o(x)/a}\right)^2\right]$. We now assume that the surviving first generation electrons hit the screen wall *instantaneously* after the passage of the next bunch. Combining their energy gain $W(x,y) = \varepsilon_{\max}a^2y^2/(x^2+y^2)^2$, in kick approximation and in presence of a vertical magnetic field, with the secondary electron yield given by Eq. (4), we thus get the 'second generation' electron surface density

$$n_1(x) = \int_{-y_o(x)}^{y_o(x)} {\rm d}y\, \delta_{\rm SEY}(W(x,y),\theta(x))\, n_{\rm e}(x,y,t_{\rm sep}).$$

Here $\theta(x) = \arccos(y_o(x)/a)$.

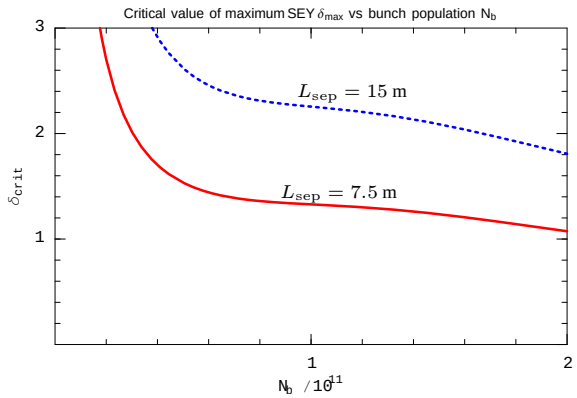

Figure 3: Minimum value of the critical secondary electron yield [39] versus bunch population for a bunch spacing of 7.5 m and 15 m, pipe radius $a = 2$ cm and secondary electron energy $W_{\rm s} = 10$ eV.

Build-up of the electron cloud will take place if $n_1(x) > n_o(x)$, i.e., if $\delta_{\max} > \delta_{\rm cr}(x)$ where

$$\delta_{\rm cr}^{-1}(x) = \int_{-y_o(x)}^{y_o(x)} {\rm d}y\, h\left(W(x,y)\right)\frac{a}{y_o(x)}\frac{n_{\rm e}(x,y,t_{\rm sep})}{n_o(x)}.$$

This defines a critical value $\delta_{\rm cr}$, weakly dependent on the horizontal position x along the beam screen cross section, for the maximum secondary electron yield: if $\delta_{\max}$ is smaller than the critical value, there is no spontaneous amplification of the electron cloud density. For nominal LHC parameters ($N_{\rm b} = 10^{11}$, $L_{\rm sep} = 7.5$ m) and assuming a typical secondary electron energy $W_{\rm s} = 10$ eV, one finds a minimum $\delta_{\rm cr}$ of about 1.35, in agreement with simulation results [40, 43]. Such a low value for $\delta_{\max}$ may not be easy to achieve, especially in the initial phase of operation until

the surface has been exposed to a sufficiently large photoelectron dose. As shown in Fig. 3, however, $\delta_{\rm cr}$ increases significantly for larger bunch spacings and has a weak dependence on the bunch population. Therefore, as a possible back-up solution, one could envisage to increase the LHC bunch spacing. In addition to low emissivity coatings, possible remedies are weak solenoid fields (only effective in the field free regions) or clearing electrodes for the low energy secondary electrons.

4 CONCLUSIONS

There has been substantial theoretical progress in the understanding of the FBII and of the Electron Cloud build-up. Comparison with experiments performed on existing machines is qualitatively satisfactory, although there are still unclear issues. The experimental diagnostic is also remarkably progressing. Simulations now agree to better than 20% for the LHC heat load; their predictive power is limited by the experimental knowledge of wall surface properties.

5 REFERENCES

[1] A. Chao, in Proc. International Workshop on Multibunch Instabilities in Future Electron and Positron Accelerators (MBI97), Tsukuba, 1997, edited by Y.H. Chin, KEK Proceedings 97-17 (1997), pp. 320–325.

[2] T.O. Raubenheimer and F. Zimmermann, SLAC-PUB-95-6740 (March 1995), Phys. Rev. **E52**, 5487–5497 (1995).

[3] G.V. Stupakov, T.O. Raubenheimer, and F. Zimmermann, SLAC-PUB-95-6805 (May 1995), Phys Rev **E52**, 5499–5504 (1995).

[4] F. Zimmermann, T.O. Raubenheimer, and G. Stupakov, SLAC-PUB-95-6792 (June 1995), in Proc. IEEE Particle Accelerator Conference (PAC95), Dallas, 1995, (IEEE, Piscataway, NJ, 1996), pp. 3102–3104.

[5] G.V. Stupakov, in Proc. International Workshop on Collective Effects and Impedance for B-Factories (CEIBA95), Tsukuba, 1995, edited by Y.H. Chin, KEK Proceedings 96-6 (1996), pp. 243–269.

[6] S.A. Heifets, SLAC PEP-II AP-Note 95-20 (July 1995) and SLAC-PUB-6959 (January 1996), in Proc. CEIBA95 (see Ref. [5]), pp. 270–282.

[7] J.M. Byrd, et. al., SLAC-PUB-7389 (December 1996), in Proc. Advanced ICFA Beam Dynamics Workshop, Arcidosso, 1996, edited by S. Chattopadhyay, M. Cornacchia and C. Pellegrini, AIP Conference Proceedings 395 (1997), pp. 175-190.

[8] J. Byrd, et. al., CERN CLIC Note 325 (January 1997), SLAC-PUB-7507 (May 1997), Phys. Rev. Letters, **79**, 79–82 (1997), and SLAC-PUB-7512 (May 1997), presented at the IEEE Particle Accelerator Conference (PAC97), Vancouver, May 1997.

[9] F. Zimmermann, et. al., SLAC-PUB-7617 (October 1997), in Proc. MBI97 (see Ref. [1]), pp. 23–31.

[10] F. Zimmermann, et. al., SLAC-PUB-7736 (January 1998), presented at the Advanced ICFA Workshop, Frascati, October 1997.

[11] H. Fukuma, et. al., presented at IEEE PAC97.

[12] X.L. Zhang, S. Kurokawa, and H. Fukuma, in Proc. MBI97 (see Ref. [1]), pp. 60–87.

[13] M. Kwon, J.Y. Huang, T.Y. Lee, M. Yoon, Y.H. Chin, H. Fukuma, KEK Report 97-6 (June 1997).

[14] M. Kwon, et. al., in Proc. MBI97 (see Ref. [1]), pp. 32–40.

[15] S. Heifets, in Proc. MBI97 (see Ref. [1]), pp. 98–109.

[16] A.W. Chao and G.V. Stupakov, SLAC-PUB-7607 (July 1997), in Proc. MBI97 (see Ref. [1]), pp. 110–116.

[17] F. Zimmermann, et. al., SLAC-PUB-7665 (October 1997), in Proc. MBI97 (see Ref. [1]), pp. 88–97.

[18] J.M. Laslett, A.M. Sessler, and D. Möhl, Nucl. Instrum. Methods **121**, 517–524 (1974).

[19] P.F. Tavares, CERN PS/92-55 (LP) (September 1992) and PhD. Thesis Univ. Campinas, SP, Brazil (November 1993).

[20] J.-M. Filhol, private communication (March 1998).

[21] K. Ohmi, Phys. Rev. Lett. **75**, 1526-1529 (1995).

[22] M. Isawa, Y. Sato, and T. Toyomasu, Phys. Rev. Lett. **74**, 5044 (1995).

[23] Z.Y. Guo, et. al., in Proc. MBI97 (see Ref. [1]), pp. 150–162.

[24] J.T. Rogers and T. Holmquist, in Proc. CEIBA95 (see Ref. [5]), pp. 322–331.

[25] M. Furman, private communication (April 1998).

[26] F. Ruggiero, World-wide web page on "Electron Cloud in the LHC", `http://wwwslap.cern.ch/collective/electron-cloud/`.

[27] F. Zimmermann, CERN LHC Project Report 95 and SLAC-PUB-7425 (February 1997),

[28] O. Gröbner, CERN LHC Project Report 127 (July 1997), presented at IEEE PAC97.

[29] J.B. Jeanneret, CERN SL/Note 97-48 (AP) (June 1997).

[30] I. Bojko, J.-L. Dorier, N. Hilleret and Ch. Scheuerlein, CERN LHC Vacuum Technical Note 97-19 (June 1997).

[31] J.S. Berg, CERN LHC Project Note 97 (July 1997).

[32] V. Baglin, I.R. Collins and O. Gröbner, contribution to these Proceedings.

[33] A.V. Burov and N.S. Dikansky, in Proc. MBI97 (see Ref. [1]), pp. 200–220.

[34] F. Zimmermann, SLAC-PUB-7664 (October 1997), in Proc. MBI97 (see Ref. [1]), pp. 221–233.

[35] M.A. Furman, LBNL-40914/CBP Note 241 (October 1997), in Proc. MBI97 (see Ref. [1]), pp. 234–246.

[36] O. Brüning, CERN LHC Project Note 102 (August 1997).

[37] I.R. Collins, A.G. Mathewson, and R. Cimino, CERN LHC Vacuum Technical Note 97-24 (September 1997), presented at ECASIA'97, Göteborg, Sweden, 16–20 June 1997.

[38] F. Caspers, J.-M. Laurent, M. Morvillo, and F. Ruggiero, CERN LHC Project Note 110 (September 1997).

[39] G. Stupakov, CERN LHC Project Report 141 (October 1997).

[40] O. Brüning, CERN LHC Project Report 158 (November 1997).

[41] F. Zimmermann, SLAC-PUB-7735 (January 1998), presented at the Advanced ICFA Workshop, Frascati, October 1997.

[42] F. Ruggiero, CERN LHC Project Report 166, (February 1998), presented at the Advanced ICFA Workshop, Frascati, October 1997.

[43] M.A. Furman, CERN LHC Project Report 180 (May 1998), also published as LBNL-41482/CBP Note 247.

[44] L. Vos, CERN LHC Project Report in preparation.

[45] H. Seiler, J. Appl. Phys. **54**, 11 (1983).